

# Design of XOR/XNOR optical logic circuit with two cascaded microring resonators and U-bend waveguides\*

ZHANG Xin (张鑫)\*\*, LI Zhi-quan (李志全), and TONG Kai (童凯)

*School of Electronic Engineering, Yanshan University, Qinhuangdao 066004, China*

(Received 9 July 2014)

©Tianjin University of Technology and Springer-Verlag Berlin Heidelberg 2014

An XOR/XNOR optical logic circuit with two cascaded microring resonators and two U-bend waveguides is proposed. The microring resonators are made of electro-optical polymer and modulated through linear electro-optical effect. Two electrical signals are applied to the two microrings, and simultaneous XOR and XNOR operations are demonstrated in two different operating modes. We also use scattering matrix method to analyze the analog output spectra, and find that different inputs like '00' and '11' can lead to different extinction ratios in output spectra at certain wavelengths, even though their digital outputs are the same.

**Document code:** A **Article ID:** 1673-1905(2014)06-0415-5

**DOI** 10.1007/s11801-014-4131-6

The traditional semiconductor Boolean logic gates usually have two input signals and only one output signal, and the inputs which determine the state of elements must pass through the preceding elements<sup>[1]</sup>. Such logic gates are not only dissipative in energy and information, but also delayed in processing time. Unlike traditional logic gates, the optical logic circuits with switching elements perform the logic operation by simultaneous independent work of each element<sup>[2]</sup>. Due to the structure design, some optical logic gates inherently carry out multiple operations at the same time<sup>[3-8]</sup>. Because of the potential advantages in the power consumption and processing speed over the traditional logic gates, optical logic circuits become a hot topic in recent researches.

In this decade, several papers have reported that microring resonator has great application in optical switch with the merits of high integration density, short response time, low power consumption, high extinction ratio, high system stability and so on<sup>[9-11]</sup>. Since the optical logic circuits consist of switching elements, microring resonators are naturally introduced in the structure design of optical logic gates. A tree structure XOR/XNOR gate with three microring resonators is reported in 2011<sup>[3]</sup>. Besides, the designs with two parallel microrings, two cascaded microrings and other structures are reported recently<sup>[4-6]</sup>.

In this paper, an XOR/XNOR logic gate with two cascaded microring resonators and two U-bend waveguides is proposed. The structure is based on directed logic circuits with two microring resonators<sup>[5]</sup>, but is optimized in some fields. The logic gates reported before usually use silicon-on-insulator (SOI) materials, and the microrings

are controlled by heaters based on the good thermo-optical effect on SOI materials<sup>[5,12]</sup>. In this paper, we use a linear electro-optical polymer to replace the SOI materials<sup>[13-15]</sup>. The electrical signal is loaded on the microring directly, and the energy transformation loss is saved. Furthermore, the room of the logic gate shrinks because the heater pad is no longer necessary. Besides, the time for temperature rise can also be saved. Despite the material, the application of two U-bend waveguides helps to remove the crossing of two straight waveguides, which can cause striking ripples in the spectra according to Ref.[5]. Based on the numerical simulations, the output spectra of designed device are analyzed by the scattering matrix method, and two different operation modes are both proved to be suitable for XOR and XNOR logic operations.

The structure of optical logic circuit is shown in Fig.1(a). Two cascaded microrings as optical switching elements with two U-bend waveguides are the core parts of the logic device. The longer U-bend waveguide picks the through signal from the first ring and adds it to the output. The shorter U-bend waveguide is used for changing the direction of light signal in the second ring to match the feedback signal from longer U-bend waveguide. The propagation direction of signal light follows the arrows in Fig.1(a). In this logic circuit, two logic signals of  $X$  and  $Y$  are used to control the states of two microrings. First of all, we assume that the resonant wavelengths of microrings are equal to the wavelength of signal light if control signals  $X$  and  $Y$  are at high level (represented as 1). On the other hand, if the control signals  $X$  and  $Y$  change to the low level (represented as 0), the resonant

\* This work has been supported by the National Natural Science Foundation of China (No.61172044), and the Natural Science Foundation of Hebei Province (No.F2012203204).

\*\* E-mail: owen88zjnbzhx@126.com

wavelengths of microrings shift, and the output intensity in particular wavelength also changes completely to the opposite according to the theory of microring switch<sup>[16]</sup>. Then we define the high intensity level of particular wavelength in output port as logic 1 and the low intensity level as logic 0. Based on these rules, we can calculate the output signal through logic operation as follows. Firstly, the input signal at particular wavelength gets through the top coupling section of X ring. If the control signal is 1, since the resonant wavelength equals the wavelength of signal, the light signal will be all coupled into the ring. Therefore, the intensity of light in through port is at low level (represented as 0), and the intensity in drop port is at high level (represented as 1). Based on the theory of microring switch, we can conclude that the logic signal in through port is  $\bar{X}$  and that in the drop port is  $X$ . Secondly, the signal gets through the top coupling section of Y ring. The signal  $X$  becomes  $X\bar{Y}$ . Meanwhile, the signal  $X$  dropping from ring Y becomes  $XY$ . Thirdly, because of the U-bend signal, the light signal  $\bar{X}$  which gets through the top coupling section of X ring is picked up and added into the bottom coupling section of Y ring. The signal  $\bar{X}$  gets through the bottom coupling section and becomes  $\bar{X}\bar{Y}$ , meanwhile the signal  $\bar{X}$  goes upstairs through the ring Y and becomes  $\bar{X}Y$ . Finally, we add the two parts of signal and obtain output signal in two output ports, which are  $X\bar{Y} + \bar{X}Y$  in output1 and  $XY + \bar{X}\bar{Y}$  in output2. Those two signals are just the results of XOR and XNOR operations. On the math level, our structure is proved to be feasible as a logic device.

In this structure, we use electro-optic polymer to make the microring. The cross section of ring waveguide is shown in Fig.1(b). The ring waveguide consists of two electrodes, two confined layers and electro-optic core material. The voltage difference between two electrodes determines the effective index of microring. Based on the electro-optic modulation theory, the relationship between effective index variation and input voltage is expressed as

$$\Delta n_{10} = \frac{1}{2} n_{10}^3 r_{33} E_1 = \frac{n_{10}^3 n_{20}^3 r_{33} U}{2(2n_{10}^2 d_2 + n_{20}^2 d_1)}, \quad (1)$$

where  $n_{10}=1.59$  is the refractive index of electro-optic polymer material,  $n_{20}=1.461$  is the index of confined layer,  $r_{33}=68$  pm/V is the electro-optic coefficient,  $U$  is the input voltage, and  $d_1=1.7$   $\mu\text{m}$  and  $d_2=2.5$   $\mu\text{m}$  are the thicknesses of core material layer and confined layer, respectively.

The other parameters are defined as follows: the radii of microrings are  $R=10$   $\mu\text{m}$ , the gaps between ring and channel waveguides are 800 nm, the length of short U-bend waveguide is  $L_1=2\pi R$  and the length of long U-bend waveguide is  $L_2=6\pi R$ , the bend losses of two U-bend waveguides are  $\alpha_{L1}=0.25$  dB/cm and  $\alpha_{L2}=0.15$  dB/cm, the bend loss of ring waveguide is  $\alpha_R=0.3$  dB/cm, and the loss of straight waveguide is ignored.

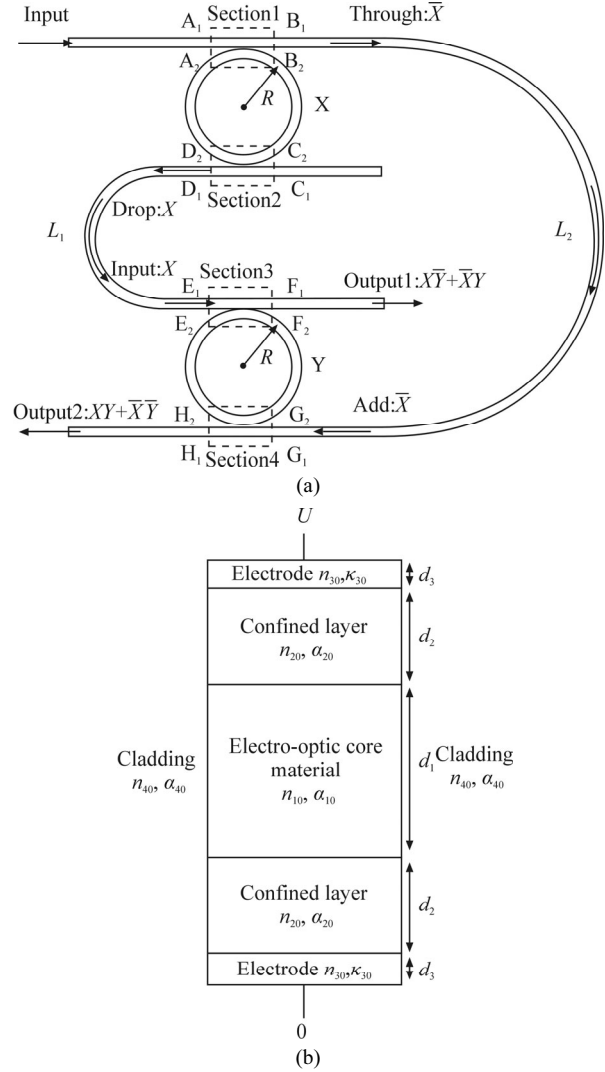


**Fig.1 (a) Schematic diagram of the designed XOR/XNOR logic circuit with two microrings and two U-bend waveguides; (b) Cross section of the microring**

Based on the transfer matrix and coupling mode theory, the output spectrum of this structure can be obtained by<sup>[17]</sup>

$$\left| \frac{F_1}{A_1} \right|^2 = \left| \frac{[\exp(2j\varphi_R) - 1]t[k^4 \exp(j\varphi_L) + (t^2 - 1)^2 \exp(j\varphi_L)]}{k^4 [t^2 \exp(2j\varphi_R) - 1]} \right|^2, \quad (2)$$

$$\left| \frac{H_1}{A_1} \right|^2 = \left| \frac{k^4 [\exp(2j\varphi_R) - 1]t^2 \exp(j\varphi_L)}{k^6 [\exp(2j\varphi_R)t^2 - 1] \exp(j\varphi_R)} + \frac{[\exp(2j\varphi_R) - 1]^2 t^2 (t^2 - 1)^2 \exp(j\varphi_L)}{k^6 [\exp(2j\varphi_R)t^2 - 1] \exp(j\varphi_R)} - \frac{k^2 [\exp(2j\varphi_R) - t^2] (t^2 - 1)^2 \exp(j\varphi_R + j\varphi_L)}{k^6 [\exp(2j\varphi_R)t^2 - 1] \exp(j\varphi_R)} \right|^2, \quad (3)$$

where  $t$  and  $k$  are amplitude transmission coefficient and

amplitude couple coefficient, respectively, and  $k^2+r^2=1$ . The transfer phase factors are  $\varphi_R = \pi R(\beta - j\alpha_R)$ ,  $\varphi_{L_1} = L_1(\beta - j\alpha_{L_1})$  and  $\varphi_{L_2} = L_2(\beta - j\alpha_{L_2})$ , where  $\beta$  is the propagation constant, and  $\alpha_i$  is the loss coefficient.

In this simulation, we use two tunable voltage sources to drive the electro-optical polymer microrings. The refractive indices of microring waveguides increase, and the resonant wavelength red shifts accordingly.

First of all, the broadband light is coupled into the device as the source. Therefore, we can determine the work wavelength of light signal for logic circuits by the aid of output spectrum analysis. The work wavelength can be chosen in two different ways, which are locating in on-resonant wavelength and off-resonant wavelength. According to the simulations shown in the next two subsections, both operation modes can satisfy the logic operations of XOR and XNOR.

Fig.2 shows the output spectra of two output ports when  $X$  and  $Y$  are in different logic values. When neither of the two microrings is on-load as shown in Fig.2(a), a deep valley can be found in the middle of the resonant peak. The bottom of the valley is about 12.1 dB. We consider that the output intensity is at the low level as logic 0 in the valley bottom. On the contrary, the light intensity at the same wavelength in the spectrum of output port 2 is  $-3.5$  dB. Similarly, we consider this maximum as the high level as logic 1. Judging from Fig.2(a), we choose the resonant wavelength of  $1.513\ 675\ \mu\text{m}$  as the work wavelength, at which both microrings are resonant without input voltage. According to Eq.(1), we can add a drive voltage of  $51.8\ \text{V}$  to increase the refractive index of  $0.001$  in microring waveguides. If the drive voltage of  $51.8\ \text{V}$  is considered as the high level (represented as logic 1), we can determine the analog output intensity representing for logic 1 in the other three situations in Fig.2. In Fig.2(b), the drive voltage is only applied on microring  $X$  to make its resonant waveguides red-shift to  $1.514\ 63\ \mu\text{m}$ . The intensities at work wavelength are  $-2.1$  dB (represented as logic 1) in output1 and  $-16.1$  dB (represented as logic 0) in output2. Ignoring the constant errors, when the voltage is only applied on microring  $Y$ , the output spectra shown in Fig.2(c) are the same with those in Fig.2(b). Finally, when the voltage is applied on both microrings, the light intensities at work wavelength are less than  $-20$  dB (represented as logic 0 in low level) in output1 and almost  $0$  dB (represented as logic 1 in high level) in output2.

After the work wavelength of logic gates is chosen through the analysis of output spectra, we change the source from broadband signal light to monochromatic light at work wavelength. Before the binary signal is added on the microring, we should calculate the time of switch response. For every single ring in this circuit, the rising time and the falling time of switch response are approximately  $0.2\ \text{ps}$ . For the whole circuit, the switch response time should be plus the delay in waveguides. It costs signal light  $0.2\ \text{ps}$  to travel through the short U-bend

waveguide and  $0.6\ \text{ps}$  to travel through the long U-bend waveguide. If we suppose the output waveguide is  $200\ \mu\text{m}$ , the response times of output1 and output2 are  $1.6\ \text{ps}$  and  $2\ \text{ps}$ , respectively. The switch response time of the whole circuit is  $2\ \text{ps}$ , and the operation rate of logic gate can reach  $500\ \text{Gbit/s}$  on theory. This response time is much shorter than that of the SOI logic gates reported before.

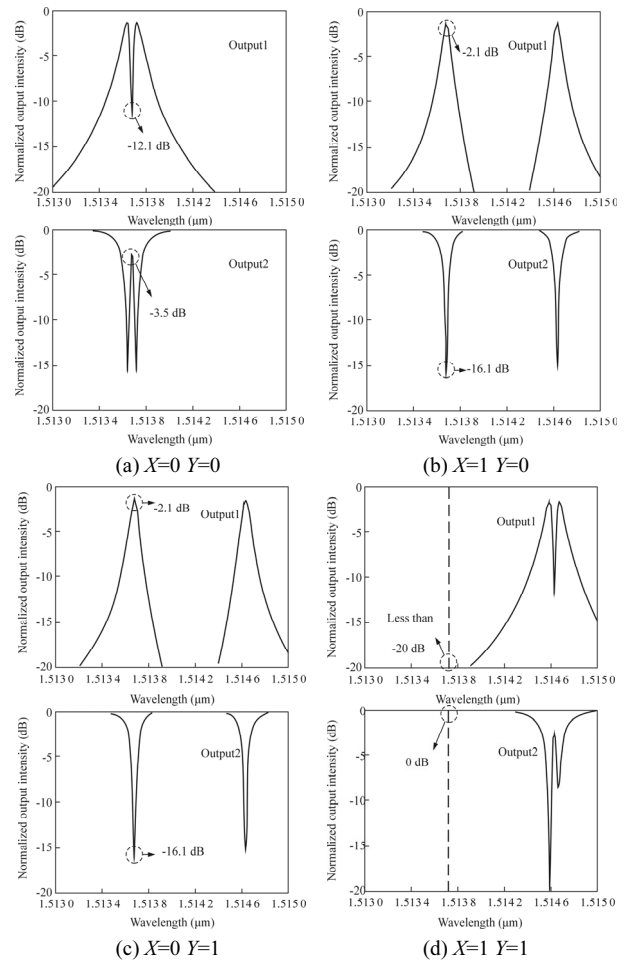


**Fig.2 Output spectra of two output ports in different situations for selecting the work wavelength in on-resonant region**

Then we build a mathematic model of logic circuit and simulate it by Simulink. Two binary electrical signals shown in Fig.3(a) and (b) are loaded on the microrings  $X$  and  $Y$ . The voltage of  $58\ \text{V}$  is represented as 1, and the voltage of  $0\ \text{V}$  is represented as 0. The simulation results are displayed in Fig.3(c)–(f). Compared with the intensity of input signal, the normalized intensities of two output ports in  $2\ \text{ns}$  are described in Fig.3(c) and (e). In Fig.3(c), two negative spikes appear at  $0.05\ \text{ns}$  and  $1.95\ \text{ns}$  because the speed limits transitions of the microrings. At these time slots, electrical signal  $X$  changes from 1 to 0, and the other signal  $Y$  changes from 0 to 1. According to the simulation of output ports, negative spikes appear at output1, and positive spikes appear at output2. If we define the normalized analog intensity in output ports as

logic 0 with value below 0.3 and logic 1 with value above 0.7, the logic outputs of two output ports are shown in Fig.5(d) and (f). It is obvious that the output digital signals of output1 and output2 equal the logic operation results of XOR and XNOR, respectively. Because of the bend loss in U-bend waveguide and rings, as shown in Fig.3(a) and (d), the output intensity has obvious difference when the work wavelength is on or off the resonance region. As a result, the output intensity at those time slots with electrical signals on microrings both at 1 has obvious difference with signals both at 0. For example, in Fig.3, at the time slot from 0.15 ns to 0.2 ns, both voltage signals are 0, and the normalized output intensities are 0.3 in output1 and 0.7 in output2. If we focus on another time slot between 0.3 ns and 0.4 ns, when the voltage signals are at 1, the normalized output intensities are 0.05 at output1 and 0.95 at output2. Although the intensity difference between these two situations is ignored by digitization, it is still an obvious difference in analog output intensity. If we have the analog signal, it is easy to tell this “0” at output is from two “1s” input or two “0s” input.

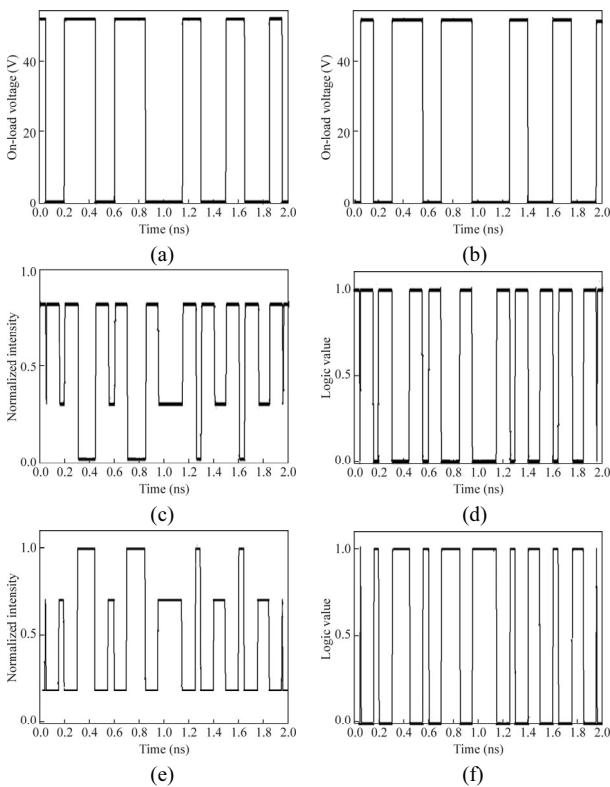


**Fig.3 Simulation results for the case of working in the on-resonant region: Electrical signals applied on (a) microring X and (b) microring Y; Normalized intensity outputs of (c) output1 and (e) output2; Logic outputs of (d) output1 and (f) output2**

In this operation mode, as shown in Fig.4, we choose the work wavelength of monochromatic light source not at the resonant wavelength when both electrical signals are at low level. The work wavelength is 1.514 62  $\mu\text{m}$  in

this case. When the logic values in microrings are  $X=0$  and  $Y=0$ , the light intensity in output1 is less than 20 dB (low level, logic 0), while the light intensity in output2 is nearly 0 dB (high level, logic 1). If one of the electrical signals changes to 1, according to Fig.4(b) and (c), the light intensity at work wavelength is up to 2.2 dB (high level, logic 1) in output1, and its counterpart in output2 reaches the bottom of 15.2 dB (low level, logic 0). In Fig.4(d), there is a spike at the work wavelength in the middle of resonant peak. We consider the bottom intensity of -12.1 dB in output1 as logic 0 and the peak intensity in output2 as logic 1.

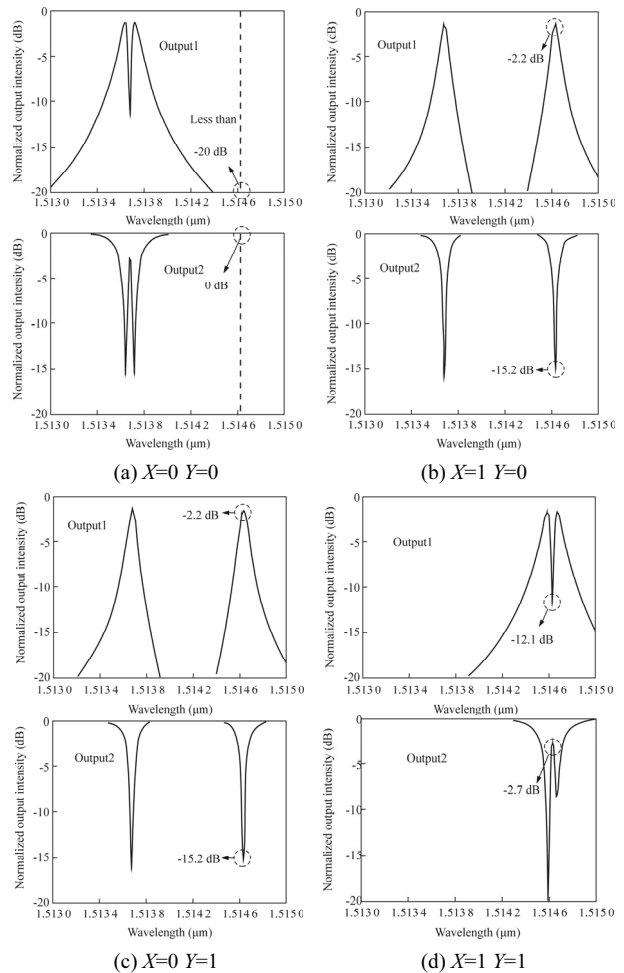


**Fig.4 Output spectra of two output ports in different situations for selecting the work wavelength in off-resonant region**

Based on the same principle explained above, output simulation results of two output ports are shown in Fig.5. Fig.5(a) and (b) are the electrical signals loaded on two microrings. Fig.5(c) shows the normalized intensity in output1 through the whole time range of 2 ns. At the time slot of 0.05 ns, when X changes from 0 to 1 and Y changes from 1 to 0, the spike appears because of the limited transition speed. When both X and Y are 0, for example, from 0.15 ns to 0.2 ns, the analog normalized output intensity in output1 is around 0.1, which is repre-

sented as logic 0. When both  $X$  and  $Y$  are 1, for example, from 0.3 ns to 0.45 ns, the analog output intensity in output1 is around 0.28, which is also represented as logic 0. Although these two situations have the same output logic value, the analog intensities have obvious difference. Fig.5(d) shows the output logic value at output1 port. Fig.5(e) and (f) show the analog and digital output intensities of output2 during 2 ns. According to Fig.5, it is obvious that the device performs well as a logic circuit for XOR and XNOR operations.

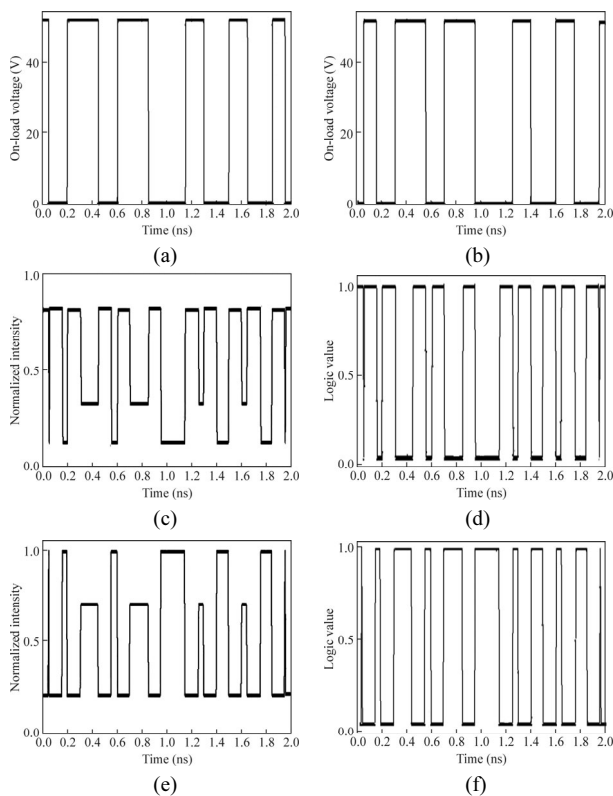


**Fig.5 Simulation results for the case of working in the off-resonant region: Electrical signals applied on (a) microring X and (b) microring Y; Normalized intensity outputs of (c) output1 and (e) output2; Logic outputs of (d) output1 and (f) output2**

When the work wavelength is in the on-resonance region, the output intensity in the situation of  $X=0$  and  $Y=0$  is higher than that in the situation of  $X=1$  and  $Y=1$  in output1. However, when the work wavelength is in the off-resonance region, the output intensity in the situation of  $X=0$  and  $Y=0$  is lower than that in the situation of  $X=1$  and  $Y=1$  in output1. It is a good mark to distinguish whether the work wavelength is in on- or off-resonance region when no voltage is applied on microrings.

To achieve faster operations and higher integration

density, we propose an optical logic circuit with two cascaded microrings and two U-bend waveguides. Simultaneous XOR and XNOR operations are implemented, and the simulation of bitwise operations is demonstrated in two different operation modes using linear electro-optic modulation. The output spectra are analyzed through numerical simulations, and the analog output signal is demonstrated as well. Because of the different lengths of U-bend waveguides, we can deduce the different states of inputs by analog spectra when their digital outputs are the same.

## References

- [1] J. Hardy and J. Shamir, *Optics Express* **15**, 150 (2007).
- [2] H. J. Caulfield and S. Dolev, *Nature Photonics* **4**, 261 (2010).
- [3] Muhammad Arif Jalil, Iraj Sadgh Amiri, Chat Teeka, Jalil Ali and P. P. Yupapin, *Physics Express* **1**, 15 (2011).
- [4] Yonghui Tian, Lei Zhang, Ruiqiang Ji, Lin Yang and Ping Zhou, *Optics Letters* **36**, 1650 (2011).
- [5] Lei Zhang, Jianfeng Ding, Yonghui Tian, Ruiqiang Ji and Lin Yang, *Optics Express* **20**, 11605 (2012).
- [6] Lei Zhang, Ruiqiang Ji, Yonghui Tian, Lin Yang and Ping Zhou, *Optic Express* **19**, 6524 (2011).
- [7] Jayanta Kumar Rakshit and Jitendra Nath Roy, *Optics Communications* **321**, 38 (2014).
- [8] Jitendra Nath Roy and Jayanta Kumar Rakshit, *Optics Communications* **312**, 73 (2014).
- [9] I. S. Amiri and J. Ali, *Quantum Matter* **2**, 116 (2013).
- [10] Sooraj Ravindra, Arnab Datta, Kmal Alameh and Yong Tak Lee, *Optics Express* **20**, 15610 (2012).
- [11] Hiroki Ikehara, Tsuyoshi Goto, Hiroshi Kamiya, Taro Arakawa and Yasuo Kokubun, *Optics Express* **21**, 6377 (2013).
- [12] Ren Guang-Hui, Chen Shao-Wu and Cao Tong-Tong, *Acta Physica Sinica* **61**, 034215 (2012). (in Chinese)
- [13] Yan Xin, Ma Chunsheng, Chen Hongqi, Zheng Chuantao, Wang Xianyin and Zhang Daming, *Acta Optica Sinica* **29**, 2540 (2009). (in Chinese)
- [14] Zhuoni Fan, BinFeng Yun, Guohua Hu, Yijian Yan and Yiping Cui, *Journal of Optoelectronics-Laser* **23**, 1727 (2012). (in Chinese)
- [15] Liang Lei, Qu Lucheng, Zhang Lijun, Zheng Chuantao, Sun Xiaoqiang, Wang Fei and Zhang Daming, *Journal of Optoelectronics-Laser* **25**, 642 (2014). (in Chinese)
- [16] Lin Xu, Wenjia Zhang, Qi Li, Johnie Chan, L. R. Hugo, M. Lipson and K. Bergman, *IEEE Photonics Technology Letters* **24**, 473 (2012).
- [17] Ying Lu, Xiangyong Fu, Danping Chu, Wuqi Wen and Jianquan Yao, *Optics Communications* **284**, 476 (2011).